

Formation and propagation of shock waves in the conduction channel of a field-effect-transistor structure

S. Rudin

U.S. Army Research Laboratory, Adelphi, Maryland 20783

G. Samsonidze

A. F. Ioffe Physical Technical Institute, St. Petersburg, 191040 Russia

(Received 9 June 1998)

We consider the evolution of a nonuniform initial electron-density distribution in the conduction channel of a field-effect-transistor structure using a hydrodynamic description which is a reasonable approximation for devices with high electron densities and short gate lengths. We show that nonlinear terms in the hydrodynamic equations may lead to the formation of the shock waves in the quasi-two-dimensional electron gas in the conduction channel, and study how their propagation is affected by the boundary conditions on the source and drain sides of the channel. For the time-independent boundary conditions considered in this work, nonlinear effects such as shocks will decay with time as energy is dissipated at the shock front. However, these examples will help us to understand nonlinear effects in the response of two-dimensional electron gas to high-frequency signals. In that situation the nonlinear waves will persist even when dissipation is significant.

[S0163-1829(98)04848-6]

I. INTRODUCTION

In a field-effect transistor (FET) the equilibrium density of electrons n_0 in the conduction channel is proportional to the average gate "voltage swing" U_0 defined as the difference between the gate-to-channel voltage and the threshold voltage. As a result of the screening by the gate electrode the dispersion law for plasma waves in the conduction channel is linear, and the velocity of small amplitude waves is determined by the gate voltage swing, $s_0 = (eU_0/m)^{1/2}$, where m is the electron effective mass and $-e$ is electron charge. Recently Dyakonov and Shur studied plasma resonance properties in a short (submicron) FET and proposed electronic devices operating in the terahertz frequency range.^{1,2} For the boundary conditions of their detector, i.e., a short circuit on the source side of the channel and an open circuit on the drain side, the plasma resonance frequency is $\omega_0 = \pi s_0/2L$ where L is the channel length.²

In the case of GaAs high-electron-mobility transistors (HEMT's), for gate lengths from 1 to 0.1 μm and a gate voltage swing $U_0 = 1\text{V}$, the resonance frequency ω_0 varies from 0.5 to 5 THz. For typical electron densities of the order of 10^{12} cm^{-2} in a short-channel HEMT, the electron-electron collision times can be much smaller than the collision times with impurities and phonons.¹ Under such conditions, hydrodynamic analysis shows that the linear plasmons may become unstable when the density and electric-field variations in the channel are not small.¹ Then interesting nonlinear effects appear in the device response. These nonlinear effects were treated in the perturbation approximation in Ref. 2. Results of recent measurements of a response of a GaAs HEMT used as a detector of microwave radiation³ were consistent with nonlinear plasma response theory² applied at a frequency much smaller than ω_0 . The perturbation treatment of Ref. 2 is suitable only for small-amplitude density variations. For larger amplitudes, various nonlinear wave phe-

nomena similar to hydraulic jumps and soliton propagation in hydrodynamics of fluids^{4,5} may exist in the quasi-two-dimensional (2D) electron gas in a FET structure.

In this work we will study how the hydrodynamically nonequilibrium initial conditions in a bounded electron system lead to the formation and propagation of nonlinear plasma waves. In particular, this formulation provides a convenient example to study how the presence of the boundaries affects propagation of shock waves in a gated 2D plasma. In this study we do not include the effects of external friction arising from collisions with phonons and impurities, and consider only the symmetric boundary conditions at the source and drain sides of the channel.

A study of shock wave propagation in a bounded 2D electron gas is useful because of the role that the shock waves may play in a more realistic modeling of FET devices operating at high frequencies. For example, we found that in the short-channel HEMT-based high-frequency detector recently discussed in the literature,^{2,3} the magnitude of the induced drain-to-source voltage near the plasma resonance is significantly different from the one obtained in perturbation treatment.⁶ The difference is significant in the same range of wave amplitudes where the shock waves appear and propagate in the channel.

In Sec. II we formulate the hydrodynamic equations for one-dimensional flow of the electron gas in a FET channel and consider two sets of boundary conditions. In Sec. III we present the results of the numerical solution of the hydrodynamic equations for different boundary conditions, and see how the presence of shocks in a bounded system affects the decay of the plasma waves in time. The numerical method is the well known Lax-Wendroff algorithm,^{7,8} which is adapted here to a system with two boundaries. We checked the reliability of the numerical method in the analytically solvable case of a system of nonlinear equations similar to the hydrodynamic equations of a FET plasma. This test system will be described in the Appendix.

II. HYDRODYNAMIC MODEL FOR ELECTRON MOTION IN A 2D CONDUCTION CHANNEL

The hydrodynamic description of a 2D electron plasma in semiconductor systems has been used to study confinement⁹ and scattering¹⁰ of plasmons within the linear approximation of the hydrodynamic equations, referred to as acoustics in the literature.⁴ The equations are derived as mass, momentum, and energy balance equations.⁴ Application of these equations to the one-dimensional flow of the high-density electron gas in conduction channels of FET's was suggested in Ref. 1.

Consider a narrow conduction channel of length L , separated by a distance d from the gate electrode. Let $n(r,t)$ be the 2D density of electrons in the channel, where r is the 2D position vector in the (x,y) plane, with the x axis chosen along the channel and the y axis across the channel. In FET's the width of the conduction channel is much larger than the length. The flow is described by three balance equations, which in the absence of friction and viscosity can be written as follows:

$$\frac{\partial n}{\partial t} + \frac{\partial}{\partial x} (nv) = 0, \quad (1)$$

$$\frac{\partial}{\partial t} (nv) + \frac{\partial}{\partial x} (nv^2) = -\frac{1}{m} \frac{\partial p}{\partial x} - \frac{en}{m} \frac{\partial U}{\partial x}, \quad (2)$$

$$\frac{\partial}{\partial t} (n\varepsilon) + \frac{p}{m} \frac{\partial v}{\partial x} + \frac{\partial}{\partial x} (n\varepsilon v) = 0, \quad (3)$$

where $U(x,t)$ is the gate to channel voltage, p is the pressure defined here as a force per unit width, and ε is the internal (thermodynamic) energy of the electron gas. The internal energy is given in the equation of state as a function of n and p :

$$\varepsilon = \varepsilon(p, n). \quad (4)$$

The electric potential in the channel is determined through the three-dimensional Poisson's equation. When the scale of the electric potential variations in the channel is much greater than the gate-to-channel separation d , the solution of the Poisson's equation can be obtained self-consistently in the "gradual channel" approximation¹

$$U(x,t) = \frac{e}{C} n(x,t), \quad (5)$$

where C is the gate capacitance per unit area. This approximation leads to a neglect of higher-order terms in the dispersion law.^{11,12} We substitute Eq. (5) into Eq. (2), which, with the use of continuity equation (1), can be rewritten in the form of Euler's equation.⁴

In the linear approximation the solutions are acoustic waves with the following dispersion relation between frequency ω and wave number k :

$$\omega(k) = \pm k(s_0^2 + s_a^2)^{1/2}, \quad (6)$$

where s_0 is a plasma velocity derived from the electric-field term in Eq. (2), and s_a is the speed of sound derived from the pressure gradient term. The value of s_0 is found from s_0^2

$= n_0 e^2 / mC = eU_0 / m$. The speed of sound can be found from the inverse compressibility of the electron gas which depends on the number of degrees of freedom in the internal kinetic motion. We estimate s_a^2 from the Fermi velocity of the 2D gas¹⁰ as $s_a^2 = 3u_F^2/4$.

Consider, as an example, a GaAs HEMT. Then $m = 0.067m_0$. For gate voltage $U_0 = 1$ V we obtain $s_0 = 1.62 \times 10^8$ cm/s, $n_0 = 1.94 \times 10^{12}$ cm⁻², and $s_a = 0.446 \times 10^8$ cm/s. Therefore $s_a^2/s_0^2 = 0.086$, and the contribution of the pressure gradient term in Eq. (2) is relatively small compared to the contribution of the self-consistent electric-field term. Then Eqs. (1) and (2) decouple from Eqs. (3) and (4), and can be written in the following forms:

$$\frac{\partial n}{\partial t} + \frac{\partial}{\partial x} (nv) = 0, \quad (7a)$$

$$\frac{\partial}{\partial t} (nv) + \frac{\partial}{\partial x} (nv^2) + \frac{s_0^2}{2n_0} \frac{\partial n^2}{\partial x} = 0. \quad (7b)$$

For a continuous flow we can use the first of these equations in the second one to obtain Euler's equation

$$\frac{\partial v}{\partial t} + v \frac{\partial v}{\partial x} + \frac{s_0^2}{n_0} \frac{\partial n}{\partial x} = 0. \quad (8)$$

Equations (7) and (8) are nonlinear. As a result, when a compression wave develops from an initial nonuniform density profile there will appear a shock wave propagating in the channel. The hydrodynamic variables on the two sides of the discontinuity, or a shock front, are related by jump conditions. These are obtained by integrating the conservation equations (7) over a small interval containing the discontinuity.⁵

Following Ref. 5, let us use indices 1 and 2 to label the values of the hydrodynamic variables just in front of and behind the shock. We define a jump of variable U as

$$[U] \equiv U_2 - U_1, \quad (9)$$

and from Eqs. (7) obtain the jump conditions

$$-u[n] + [nv] = 0, \quad (10)$$

$$-u[nv] + \left[nv^2 + \frac{s_0^2}{2n_0} n^2 \right] = 0,$$

where u is the shock's velocity defined as $u = dx_s(t)/dt$, $x_s(t)$ being the position of the shock front.

III. NONLINEAR WAVES IN A FET CHANNEL OBTAINED FROM HYDRODYNAMIC EQUATIONS

Various numerical methods have been developed in hydrodynamics to study flows containing shock waves, or hydraulic jumps. Because we do not include viscosity terms in Euler's equation, the resulting shocks have a theoretically zero width but finite height. We use the Lax-Wendroff numerical method⁸ developed to study discontinuous time-dependent solutions of hyperbolic systems of nonlinear conservation laws like Eqs. (7). The solutions satisfy jump conditions across the discontinuity, referred to as Rankine-

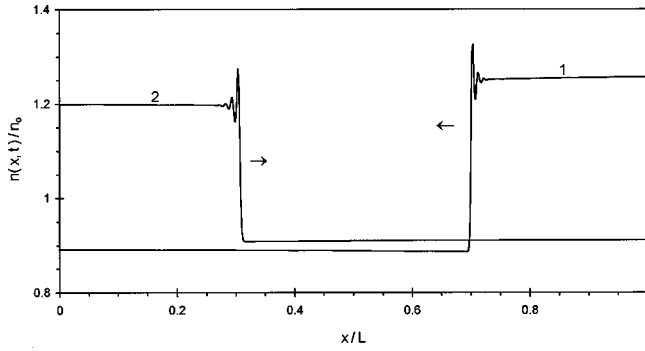


FIG. 1. Density profiles at two different times $t_1/T=2.8$ and $t_2/T=3.8$ for the open-circuit boundary conditions. T is a characteristic time defined as a ratio of the channel length L to the linear plasmon velocity s_0 . Each profile is a compression wave containing a shock front propagating in a direction indicated by an arrow.

Hugoniot relations in the mathematics literature.⁸ The relevant discussions of the stability of this numerical scheme can be found in Refs. 7 and 8. We adapt the Lax-Wendroff method to the case of one-dimensional flow in a system with two boundaries, and consider two different sets of boundary conditions.

Open circuit boundary conditions

These boundary conditions are the conditions of zero velocity at the source and drain end of the channel,

$$v(L,t)=v(0,t)=0, \quad (11)$$

and we choose the initial condition

$$n(x,0)=n_0 \times (1+A \cos \pi x/L), \quad v(x,0)=0, \quad (12)$$

where A is a dimensionless amplitude.

Define a characteristic time scale as $T \equiv L/s_0$. The time it takes a discontinuity to appear in the compression wave depends on the value of the initial amplitude A . The resulting density and velocity profiles are shown in Figs. 1 and 2 for $A=0.5$. The shallow rapid oscillations near the discontinuity are numerical artifacts that always appear in finite-difference approximations of a nonviscous flow.⁷ The shock forms at time $t < T$, and afterward the flow can be described as successive reflections of the shock wave at the left and right boundaries.

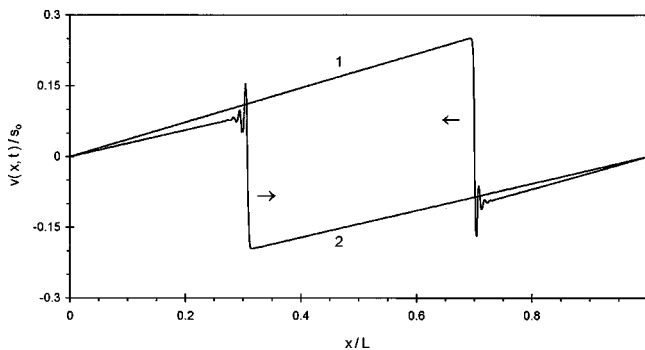


FIG. 2. Velocity profiles for the open-circuit boundary conditions at the same times as in Fig. 1.

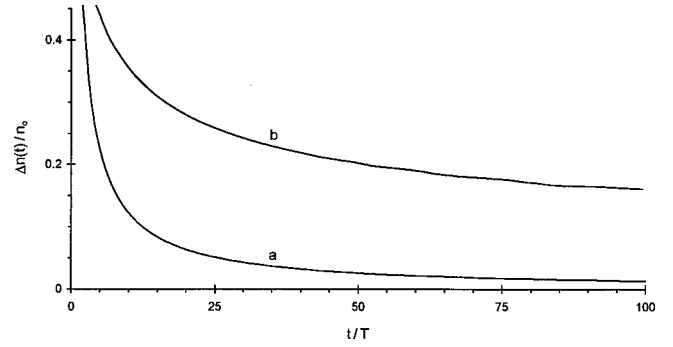


FIG. 3. (a) The magnitude of the shock as a function of time for open-circuit boundary conditions. It is defined as a difference Δn of the density values behind and in front of the shock. At large times it decays as $1/t$. (b) The envelope of the amplitude of the waves as a function of time for the constant potential boundary conditions. In this case Δn is defined as an absolute value of the maximum deviation from the equilibrium density n_0 .

In accordance with the general properties of shock waves⁴ the shock's velocity u satisfies an inequality

$$v_1 + s_1 < u < v_2 + s_2, \quad (13)$$

where indices are assigned as in Eq. (9), and

$$s^2(x,t) = \frac{s_0^2}{n_0} n(x,t). \quad (14)$$

After the initial profile is transformed into a propagating shock wave the flow is a sequence of reflections of one shock wave whose amplitude decays with time. The time interval between two successive reflections is exactly $T=L/s_0$ even after many reflections. The magnitude of the shock, defined as $\Delta n(t)=n_2(t)-n_1(t)$, decays asymptotically as $1/t$, as shown in Fig. 3(a). The decay of shocks is a well-known generic phenomenon⁴ related to energy dissipation at the shock front. The particular law of decay depends on the boundary conditions. For example, a single shock wave in an unbounded flow⁴ decays as $1/\sqrt{t}$. The presence of the reflecting boundaries leads to a different time dependence $1/t$, which is similar to the decay of a periodic compression wave in an unbounded flow.^{4,5}

The velocity of the shock front can be obtained from the jump conditions [Eqs. (10)] in terms of the values of the hydrodynamic variables behind the shock and in front of it. Let us apply these to the shock reflection at a boundary, say at $x=L$. A shock front approaches the boundary with a speed u_i , with the hydrodynamic variables of the flow being n_2 and v_2 behind the shock and n_1 and v_1 in front of the shock. It reflects with a different speed u_r , with the hydrodynamic variables being n_2 and v_2 in front and n_3 and v_3 behind the shock. From the boundary conditions $v_1=v_3=0$, and from Eqs. (10), we eliminate n_1 and obtain the magnitudes of u_i and u_r as positive solutions of the following cubic equations:

$$u_{i,r}^3 \mp v_2 u_{i,r}^2 - \frac{s_0^2}{n_0} n_2 u_{i,r} \pm \frac{s_0^2}{2n_0} n_2 v_2 = 0, \quad (15)$$

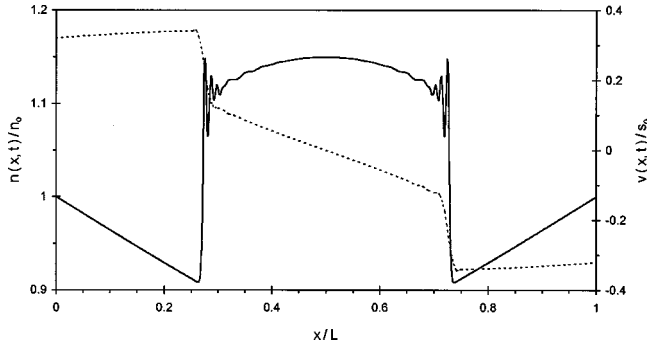


FIG. 4. Density (solid curve, left axis) and velocity (broken curve, right axis) profiles for the constant potential boundary conditions. The profiles are shown at time $t/T=3.7$. They contain two shock waves propagating toward the boundaries.

where the upper signs are to be taken for u_i and the lower for u_r . For a flow where $(v_2/s_0)^2 \ll n/n_0$, which is valid for any initial amplitude after a sufficiently large time, we can expand positive solutions of Eqs. (15) in powers of v_2 :

$$\frac{u_{i,r}}{s_0} \approx \left(\frac{n_2}{n_0}\right)^{1/2} \pm \frac{v_2}{4s_0} + \frac{5}{16} \left(\frac{v_2}{s_0}\right)^2 \left(\frac{n_0}{n_2}\right)^{1/2} \pm \dots \quad (16)$$

To the same order, the magnitude of the shock Δn changes upon the reflection instantaneously by the amount of $n_0 v^2/2s_0^2$, and then decays continuously until it is reflected from another boundary. These small instantaneous changes are not shown in Fig. 3, where only the overall decay is shown.

Constant electric potential boundary conditions

These boundary conditions are given by $U(0,t)=U(L,t)=U_0$. In the gradual channel approximation [Eq. (5)] these are replaced by

$$n(0,t)=n(L,t)=n_0. \quad (17)$$

We choose the following initial conditions:

$$n(x,0)=n_0 \times (1+A \sin \pi x/L), \quad v(x,0)=0. \quad (18)$$

After some transient time interval the two compression waves develop shocks propagating toward two boundaries, as shown in Fig. 4. After the shock fronts reach the boundaries at $x=0$ and L , the profile changes into two continuous waves, shown in Fig. 5, in which the density $n(x,t)$ is larger than the equilibrium value n_0 . The density profile then changes to the one in which n is smaller than n_0 , and then into two compression waves propagating toward the middle of the channel. Two shock fronts develop and propagate toward each other. Upon ‘‘colliding’’ at $x=L/2$ the wave transforms into two shocks propagating toward the boundaries. This sequence of profile transformations repeats after each time interval $2T$. We checked that a choice of higher harmonics in the initial conditions, Eq. (18), leads to the same profile at time $t>T$.

The magnitude of the waves, defined for this case as the maximum deviation in the interval $[0,L]$ from the equilibrium values of $n=n_0$ for the density and $v=0$ for the velocity, decreases with time. The envelope of the magnitude’s

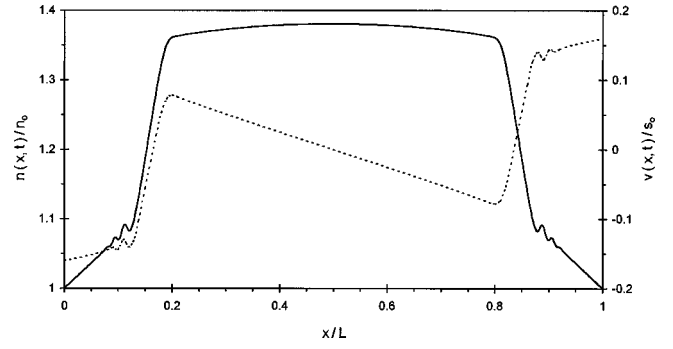


FIG. 5. Density (solid curve, left axis) and velocity (broken curve, right axis) profiles for the constant potential boundary conditions, at time $t/T=4.2$. The flow is continuous during this part of the cycle, and can be described as two waves moving toward the middle of the channel.

time dependence is shown in Fig. 3(b). At large times the decay is much slower than for the previous set of boundary conditions. We find that asymptotically the shock’s amplitude decays more slowly than $1/\sqrt{t}$.

The speed of each shock near the boundary can be expressed in terms of hydrodynamic variables behind the shock, n_2 and v_2 . For the present boundary conditions we obtain a quadratic equation for u_i , the speed of the incident shock, and find

$$\frac{u_i}{s_0} = \frac{v_2}{s_0} + \left(\frac{n_2+n_0}{2n_2} + \frac{v_2^2}{s_0^2}\right)^{1/2}. \quad (19)$$

At large times v_2 becomes small, and $u_i \approx s_0$. The reflected wave is not a compression wave and does not contain a shock until it transforms into two compression waves as described before.

APPENDIX: AN EXACTLY SOLVABLE NONLINEAR FLOW IN A BOUNDED SYSTEM

In order to test our computational method we consider a nonlinear hyperbolic system similar to Eqs. (7) and (8):

$$\frac{\partial n}{\partial t} + \frac{\partial}{\partial x} (nv) = 0, \quad (A1)$$

$$\frac{\partial v}{\partial t} + v \frac{\partial v}{\partial x} + n \frac{\partial n}{\partial x} = 0,$$

where we used dimensionless variables x/L , t/T , and v/s_0 .

In the absence of shock waves these equations describe an adiabatic flow of an ideal gas with one internal degree of freedom.⁴ The hodograph transformation⁵ which interchanges the roles of dependent and independent variables transforms these equations into linear equations for $x(n,v)$ and $t(n,v)$. These equations and the shock formation can be exactly analyzed in the case of unbounded motion with a periodic initial density profile.⁵ An exact analysis can be done also for the case of zero velocity boundary conditions

$$v(0,t)=v(1,t)=0. \quad (A2)$$

Define new hydrodynamic variables $\alpha(x,t)$ and $\beta(x,t)$:

$$\alpha = n + v, \quad \beta = n - v. \quad (\text{A3})$$

Then from Eqs. (A1) we obtain separate differential equations for α and β , and find that solutions satisfy the equations

$$\alpha = f(x - \alpha t), \quad \beta = g(x + \beta t), \quad (\text{A4})$$

where functions f and g are to be determined from the initial conditions

$$\begin{aligned} n(x,0) + v(x,0) &= f(x), \\ n(x,0) - v(x,0) &= g(x), \quad 0 \leq x \leq 1. \end{aligned} \quad (\text{A5})$$

Equations (A4) define a nonlinear mapping in α, β plane. We now choose an initial condition of zero velocity profile at $t=0$, $v(x,0)=0$. This choice of initial profile is not essential for the analysis but is a convenient one. Then $g(x)=f(x)=n(x,0)$ for $0 \leq x \leq 1$. From the boundary conditions [Eq. (A2)] we deduce then that $f(x+2)=f(x)$. Therefore, the function $f(x)$ is obtained everywhere from $n(x,0)$ defined only in the $[0,1]$ interval:

$$f(-x) = f(x) = f(x+2), \quad -\infty < x < \infty. \quad (\text{A6})$$

Let us now choose an initial profile

$$n(x,0) = 1 + A \cos \pi x, \quad (\text{A7})$$

which is equivalent to the initial conditions in Eq. (12) in dimensionless units. Then $f(x) = 1 + A \cos(\pi x)$, and its derivative is $f'(x) = -A \pi \sin(\pi x)$. The mapping in Eq. (A4) is singular when

$$[1 + t f'(x - \alpha t)] \times [1 - t f'(x + \beta t)] = 0. \quad (\text{A8})$$

From this we find that a singularity develops at time $t_s^{(0)}$ = $1/A \pi$ at the position $x_s^{(0)}$ found from the condition

$$0 \leq x_s^{(0)} = \left[2N \pm \left(\frac{1}{2} + \frac{1}{A \pi} \right) \right] \leq 1, \quad N = 0, \pm 1, \pm 2, \dots \quad (\text{A9})$$

Define a further transformation in α, β :

$$\xi = x - \alpha t, \quad \eta = x + \beta t. \quad (\text{A10})$$

For $t < t_s^{(0)}$ the flow is continuous, and in terms of these new variables it is given by the equations

$$\begin{aligned} \xi + (t - x) &= -A t \cos(\pi \xi), \\ \eta - (t + x) &= A t \cos(\pi \eta). \end{aligned} \quad (\text{A11})$$

These transcendental equations are simple to solve numerically. From $\xi(x,t)$ and $\eta(x,t)$ we can find n and v :

$$n = (-\xi + \eta)/2t, \quad v = (-\xi - \eta + 2x)/2t. \quad (\text{A12})$$

Once a shock is formed, Eqs. (A1) are not applicable because $n(\xi)$ becomes a multivalued function, but a standard shock fitting procedure⁵ can be used. The multivalued part of the density or velocity profile is replaced by an appropriate discontinuity, a jump in the hydrodynamic variable, determined by an ‘‘equal area’’ construction. This last relation is deduced from mass conservation and was treated in detail in Ref. 5 for a profile similar to our $f(\xi)$. We will use labels 1 and 2 for the values in front of and behind a shock, respectively. If the position of the discontinuity at time t is $x_s(t)$, the shock’s velocity is defined as $u = dx_s/dt$, and we obtain

$$x_s(t) = \frac{1}{2} + t, \quad u(t) = 1 \quad (\text{A13})$$

until the shock front reaches $x=1$ and reflects. The jump in α is related to the jump in ξ by an equation

$$\alpha_2 - \alpha_1 = -2A \sin[\pi(\xi_2 - \xi_1)/2]. \quad (\text{A14})$$

The shock is formed at $t = t_s^{(0)} = 1/\pi A$ with zero strength, as $\alpha_2 - \alpha_1 = 0$ at that time. It reaches its maximum strength, corresponding to $\alpha_2 - \alpha_1 = 2A$, at time $t_s^{(1)} = 1/2A$. At large times $\alpha_2 - \alpha_1 \rightarrow 2/t$ asymptotically. Correspondingly, $n_2 - n_1 \rightarrow 1/t$. This inverse linear decay of the shock strength is identical to the one we obtained numerically for the electron-gas flow in the FET conduction channel [Eqs. (7)], with open-circuit boundary conditions. However, unlike in that case, the shock here propagates with exactly the speed of linear plasma waves, s_0 in original units. We applied the Lax-Wendroff method adapted for a bounded flow to the system described by Eqs. (A1), and found numerical results to be in excellent agreement with the analytical ones.

ACKNOWLEDGMENTS

We are grateful to M. Dyakonov and F. Crowne for useful discussions. G.S. was supported by the U.S. Army European Research Office, Contract No. N68171-97-M-5548.

¹M. Dyakonov and M. Shur, Phys. Rev. Lett. **71**, 2465 (1993).

²M. Dyakonov and M. Shur, IEEE Trans. Electron Devices **43**, 380 (1996).

³R. Weikle, J. Q. Lu, M. S. Shur, and M. I. Dyakonov, Electron. Lett. **32**, 2148 (1996).

⁴L. D. Landau and E. M. Lifshitz, *Fluid Mechanics* (Pergamon, Oxford, 1978).

⁵G. B. Whitham, *Linear and Nonlinear Waves* (Wiley, New York, 1974).

⁶G. Samsonidze, S. Rudin, and M. S. Shur, in *Proceedings of the IEEE 6th International Conference on Terahertz Electronics*,

edited by P. Harrison (University of Leeds, Leeds, U.K., 1998), p. 231.

⁷P. J. Roache, *Computational Fluid Mechanics*, revised printing (Hermosa, Albuquerque, NM, 1976).

⁸P. Lax and B. Wendroff, Commun. Pure Appl. Math. **13**, 217 (1960).

⁹A. L. Fetter, Phys. Rev. B **32**, 7676 (1985).

¹⁰S. Rudin and T. L. Reinecke, Phys. Rev. B **54**, 2791 (1996).

¹¹S. Rudin and G. Samsonidze, in *Proceedings of the 4th International Semiconductor Device Resonance Symposium* (University of Virginia, Charlottesville, VA, 1997), p. 583.

¹²F. J. Crowne, J. Appl. Phys. **82**, 1242 (1997).